International Journal of Research
Available at https://edupediapublications.org/journals
p-ISSN: 2348-6848
e-ISSN: 2348-795X
Volume 03 Issue 14
October 2016

Dna Binding Studies of Cu (Ii) And Zn(Ii) Complexes of (E-2- Chloro-N- (3-Hydroxy- 5-Hydroxymethyl)- 2-Methylpyridin-4- Yl) Methylene) Acetohydrazide

Muhanad Taha Yasein
M.Sc., (Inorganic Chemistry), Department of Chemistry
Nizam College, Osmania University

ABSTRACT:
Pyridoxal chloro acetic hydrazone was synthesized by treating pyridoxal hydrochloride with chloro acetic hydrazide using EtOH as a solvent copper (II) and zinc (II) metal complexes were synthesized and characterized using, IR, U.V, LC- MS and TGA methods. IR spectra of the complex revealed the ligand coordinated through "N" and"O" donor atoms. The complexes were tested for DNA binding activity using electronic absorption spectroscopy. The interaction of metal complexes with CT-DNA was studied and the binding constant (K_b) was calculated.

Keywords: Copper (II), Chloro acetic hydrazide, DNA, Electronic absorption spectroscopy, Zinc (II) metal.

Introduction

A Schiff base is a nitrogen analog of an aldehyde or ketone in which the C=O group is replaced by C=N-R group. It is usually formed by condensation of an aldehyde or ketone with a primary amine according to the following scheme:

Where R, may be an alkyl or an ary group, Schiff bases that contain aryl substituents are substantially more stable and more readily synthesized, while those which contain alkyl substituents are relatively unstable. Schiff bases of aliphatic aldehydes are relatively unstable and readily polymerizable while those of aromatic aldehydes having effective conjugation are more stable. The formation of a Schiff base from an aldehydes or ketones is a reversible reaction and generally takes place under acid or base catalysis, or upon heating. The formation is generally driven to the completion by separation of the product or removal of water, or both. Many Schiff bases can be hydrolyzed back to their aldehydes or ketones and amines by aqueous

acid or base. The mechanism of Schiff base formation is another variation on the theme of neucleophilic addition to the carbonyl group. In this case, the neucleophile is the amine. In the first part of the mechanism, the amine reacts with the aldehyde or ketone to give an unstable addition compound called carbinolamine.

The carbinolamine loses water by either acid or base catalyzed pathways. Since the carbinolamine is an alcohol, it undergoes acid catalyzed dehydration. Typically the dehydration of the carbinolamine is the rate-determining step of Schiff base formation and that is why the reaction is catalyzed by acids. Yet the acid concentration cannot be too high because amines are basic compounds. If the amine is protonated and becomes non-neucleophilic, equilibrium is pulled to the left and carbinolamine formation cannot occur. Therefore, many Schiff bases synthesis are best carried out at mildly acidic pH. The dehydration of carbinolamines is also catalyzed by base. This reaction is somewhat analogous to the E2 elimination of alkyl halides except that it is not a concerted reaction. It proceeds in two steps through an anionic intermediate. The Schiff base formation is really a sequence of two types of reactions, i.e. addition followed by elimination. Schiff bases, named after Hugo Schiff, are formed when any primary amine reacts with an aldehyde or a ketone under specific conditions. Structurally, a Schiff base is a nitrogen analogue of an aldehyde or ketone in which the carbonyl group (C O) has been replaced by an imine or azomethine group [1].

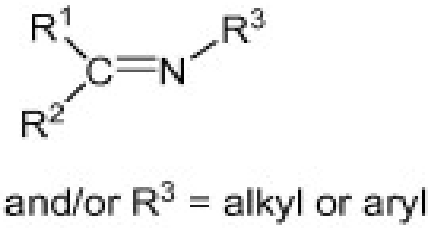

Figure 1: General structure of a Schiff Base

Schiff bases are some of the most widely used organic compounds. They are used as pigments and dyes, catalysts, intermediates in organic synthesis, and as polymer stabilizers. Schiff bases have also been shown to exhibit a broad range of biological activities, including antifungal, antibacterial, antimalarial, antiproliferative, anti-inflammatory, antiviral, and antipyretic

properties. Imine or azomethine groups are present in various natural, natural-derived, and non-natural compounds. The imine group present in such compounds has been shown to be critical to their biological activities.

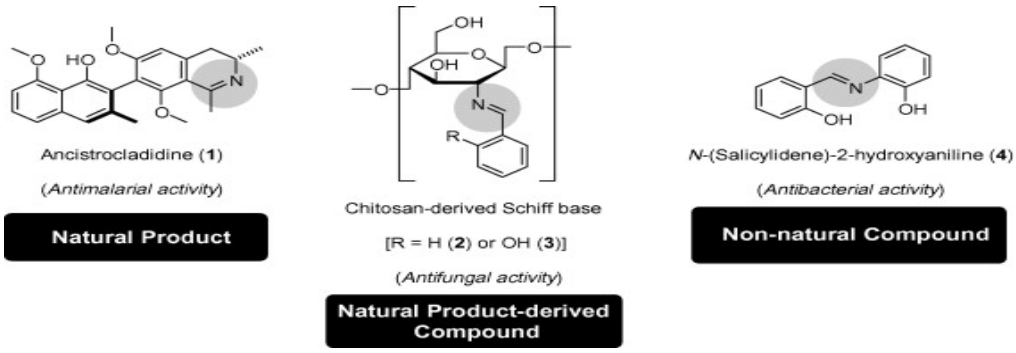

Figure 2: Examples of bioactive Schiff bases. The imine or azomethine group present in each molecular structure is shaded

In this review we present the general approaches to the synthesis of Schiff bases. We also highlight the most significant examples of compounds belonging to this class, which exhibit antimalarial, antibacterial, antifungal, and/or antiviral activities to have been reported in the literature. The relationship between Schiff bases and other pharmacological activities, such as antiproliferative activities, are not included in this review [2].

Synthesis of Schiff bases

The first preparation of imines was reported in the 19th century by Schiff (1864). Since then a variety of methods for the synthesis of imines have been described. The classical synthesis reported by Schiff involves the condensation of a carbonyl compound with an amine under azeotropic distillation. Molecular sieves are then used to completely remove water formed in the system. In the 1990s and in situ method for water elimination was developed, using dehydrating solvents such as tetramethyl orthosilicate or trimethyl orthoformate and. In 2004, Chakraborti et al. demonstrated that the efficiency of these methods is dependent on the use of highly electrophilic carbonyl compounds and strongly nucleophilic amines. They proposed as an alternative the use of substances that function as Brönsted-Lowry or Lewis acids to activate the carbonyl group of aldehydes, catalyze the nucleophilic attack by amines, and dehydrate the system, eliminating water as the final step. Examples of Brönsted-Lowry or lewis acids used for the synthesis of Schiff bases include ZnCl2, TiCl4, MgSO4-PPTS, Ti (OR) 4, alumina, H2SO4,

NaHCO3, MgSO4, Mg (ClO4)2, H3CCOOH, Er (OTf) 3, P2O5/Al2O3, HCl.In the past 12 years a number of innovations and new techniques have been reported including solvent-free/clay/microwave irradiation, solid-state synthesis, K-10/microwave, water suspension medium.

BF4/molecular sieves, infrared irradiation/no solvent, NaHSO4•SiO2/microwave/solvent-free, solvent-free/CaO/microwave and silica/ultrasound irradiation. Among these innovations, microwave irradiation has been extensively used due to its operational simplicity, enhanced reaction rates, and great selectivity. The use of microwave irradiation commenced with the independent studies of Rousell and Majetich groups. Microwave irradiation is less environmentally problematic than other methods because it abolishes the excessive use of aromatic solvents and the Dean-Stark apparatus for azeotropic removal of water [3].

BIOLOGICALACTIVITIESOF SCHIFF BASES

Antimalarial activity

Malaria is a neglected disease that still causes serious public health problems. Every year, approximately 500 million people are afflicted by the disease, of whom around 1–3 million die, 90% of who in sub-Sahara Africa are primarily children. Malaria is currently found in more than 100 countries throughout Africa, Latin America, Asia, and Oceania. Human malaria is mainly caused by four species of Plasmodium (P. falciparum, P. vivax, P. ovale, and P. malariae). The female mosquito of the Anopheles genus is the vector of Plasmodium. The search for new drugs, vaccines, and insecticides to prevent or treat this disease is clearly a priority.

Schiff bases have been shown to be interesting moieties for the design of antimalarial agents. Ancistrocladidine is a secondary metabolite produced by plants from the families Ancistrocladaceae and Dioncophyllaceae that present an imine group in its molecular scaffold. Compound 1 has been shown to be active against P. falciparum K1 and 3D7. The minimum inhibitory concentrations (MIC values) of ancistrocladidine necessary to completely abolish P. falciparum K1 and 3D7 growth were 0.3 and 1.9 µg/mL, respectively. Interestingly, compound 1 was 90- and 10-fold more selective toP. Falciparum K1 and 3D7 respectively than to rat skeletal myoblast L-6 cells. Rathelot et al. described

the synthesis of Schiff base-functionalized 5-nitroisoquinolines and investigated the in vitro activity of these compounds against an ACC Niger chloroquine resistant P. falciparum strain. Schiff base 5 was the most effective antimalarial agent among the synthesised 5-nitroisoquinoline derivatives. The concentration of compound 5 necessary to inhibit P. falciparum growth by 50% (IC50) was 0.7 µg/mL. Under the same experimental conditions the IC50 value for chloroquine was 0.1 µg/mL [4].

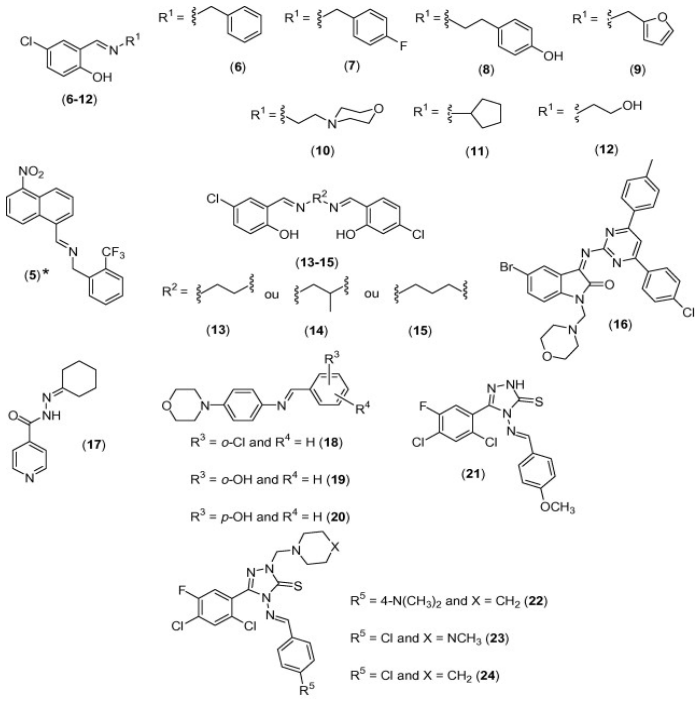

Figure 3: Chemical structure of some synthetic antibacterial Schiff bases. ∗Compound 5 is an antimalarial agent

Antibacterial Activity

The increase in the mortality rate associated with infectious diseases is directly related to bacteria that exhibit multiple resistances to antibiotics. The lack of effective treatments is the main cause of this problem. The development of new antibacterial agents with novel and more efficient mechanisms of action is definitely an urgent medical need. Schiff bases have been pointed to as promising antibacterial agents. For example, N-(salicylidene)-2-hydroxyaniline is effective against Mycobacterium tuberculosis H37Rv, exhibiting an MIC value of 8 µg/mL. The selectivity of compound4 was checked by performing experiments with J774 macrophages. No

cytotoxic effect on J774 macrophages was observed for compound 4, even when it was tested at concentrations as high as 1000 µg/mL. More than 80% of macrophage cells were viable at such experimental conditions, demonstrating the high selectivity of compound.

The synthesis and antimicrobial activity of a series of Schiff bases derived from the condensation of 5-chloro-salicylaldehyde and primary amines has recently been reported. The 5-chloro-salicylaldehyde-Shiff base derivatives were most active against at least one of the evaluated bacterial species. Pseudomonas fluorescence was the strain most sensitive to compounds, with MIC values ranging from 2.5 to 5.2 µg/mL. The MIC value for the reference drug kanamycin against the same bacterial strain was 3.9 µg/mL. The Schiff bases presented MIC values in the range of 1.6–5.7 µg/mL against Escherichia coli, while the MIC value for kanamycin was 3.9 µg/mL. Bacillus subtilis was sensitive to the Schiff base14 only (MIC = 1.8 µg/mL). The MIC values for compounds 6 and 7 againstStaphylococcus aureus were, respectively, 3.1 and 1.6 µg/mL.

Isatin-derived Schiff bases have also been reported to possess antibacterial activity. Twenty-eight bacteria of clinical interest were used in the studies performed by Pandeya and colleagues. The authors disclosed the isatin-derived Schiff base as the most potent compound amongst those synthesised against all the pathogenic bacteria studied. The MIC values for compound against E. coli NCTC 10418, Vibrio choleraenon-01, Enterococcus faecalis, Proteus shigelloides were 2.4, 0.3, 1.2 and 4.9 µg/mL. Respectively, while the MIC values for sulfamethoxazole (reference drug) against the same bacterial strains were in the range of 312–5000 µg/mL. Thus compound 16 was notably 1040-, 1040-, 4160-, and 1020-fold more potent than sulphamethoxazole. Other isatin-derived Schiff bases have been described in the literature, but with no expressive antibacterial activities [5].

The isoniazid-derived Schiff base was active against M. tuberculosis H37Rv, exhibiting an MIC value of 0.03 mg/L. In this respect, compound was slightly more potent than isoniazid, its immediate synthetic precursor. Additionally, the isoniazid-derived Schiff base was not toxic against the cell line VERO (epithelial cells from healthy monkey kidney). The IC50 for compound against VERO cells was as high as 1 g/mL, indicating that this isoniazid-derived Schiff base is selective for bacterial cells. The therapeutic safety and effectiveness for compound

is higher than 40,000, making this Schiff base an excellent lead for the development of antitubercular agents. Schiff bases with a 2, 4-dichloro-5-fluorophenyl moiety are also effective in the inhibition of bacterial growth. Schiff bases from this class completely inhibited the growth of S. aureus, E. coli, Pseudomonas aeruginosa, and Klebsiella pneumoniae. MIC values for these compounds varied from 6.3 to 12.5 μg/mL, which are comparable to those obtained for the reference drug ciprofloxacin. Madurahydroxylactone Schiff bases are imines derived from natural products. Madurahydroxylactones are secondary metabolites produced by the plant Actinomadura rubra.

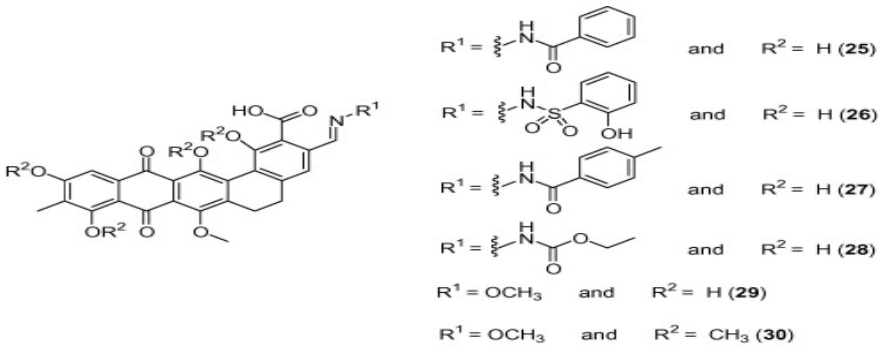

Figure 4: Examples of antibacterial Schiff bases derived from plant natural products

Other molecules of natural or non-natural origin that are platforms for the synthesis of Schiff bases for antibacterial activities include amino acids, coumarins, sulfonamides, or resacetophenones, aminothiazolyl bromocoumarins, crown ethers, O-phthaldehyde, or 2-aminophenol and 1,2,4-triazol. The antibacterial property of compounds representative of these classes was examined. However, they did not exhibit any notable activity [6].

Related work:

M. A. Neelakantan, M. Sundaram, and M. Sivasankaran Nair studied that Solution equilibria and relevant stability constants for M(II)-pyridoxine (PN)(A) [M(II) = Cu(II), Ni(II), and Zn(II)], and M(II)-PN(A)- imidazole containing ligands (B) [B = imidazole (him), benzimidazole (bim), histamine (hist), and l-histidine (his)] in aqueous solution have been determined by a pH metric method at 310 K and I = 0.15 M NaClO4. The complexation model for each system has been established by the MINIQUAD-75 program. The probable binding mode in the binary and ternary species was discussed based upon the derived stability constants. The concentration

distributions of various species formed in solution were evaluated. The stability of ternary complexes follows the Irving–Williams order of metal ions, which was quantitatively (Δ log K, log X, and % RS) compared with their corresponding binary complexes. In terms of the ligands (B), the stability of the complexes follows him. The molecular geometry of the complexes formed in solution between the ligands and M (II) was determined by electronic spectra at various pH intervals. The formation of complexes and their electrochemical properties were also assessed by cyclic voltammetry. The in vitro biological activity of the ternary complexes was tested against bacteria, fungi, and yeast.

Farukh Arjmand, , Mubashira Aziz studied that New homodinuclear macrocyclic complexes of cobalt(II), copper(II) and zinc(II) were isolated from the newly synthesized ligand 2,2,2′,2′-S,S[bis(bis- N,N-2- thiobenzimidazolyloxalato-1,2- ethane)]. The structures of the complexes were elucidated by elemental analysis, molar conductance measurements, IR, 1H NMR, 13C NMR, electronic and ESI-MS spectroscopic techniques. In complex 1, Co (II) ions possess a tetrahedral coordination environment composed of O2S2 donor atoms while it's Cu (II) and Zn (II) counterparts 2 and 3, respectively, reveal a six coordinate octahedral structure, defined by the O2S2 donors from the macrocyclic ring and two chloride ions. Molar conductance and spectroscopic data also support the proposed geometry of the complexes. DNA binding properties of complexes 1–3 were investigated using electronic absorption spectroscopy, fluorescence spectroscopy, viscosity measurements and cyclic voltammetry. The absorption spectra of complexes 2 and 3 with calf thymus DNA showed hypochromism, while complex 1 showed hyperchromism attributed to a partial intercalation and electrostatic binding modes, respectively. The intrinsic binding constant Kb of complexes 1–3 were determined as 16.6 × 104 M−1, 4.25 ×104 M−1 and 3.0 × 104 M−1, respectively. The decrease in the relative specific viscosity of calf thymus DNA with increasing concentration of the complexes authenticates the partial intercalation binding mode. Gel electrophoresis of complex 2 with plasmid DNA demonstrated that complex exhibits excellent "artificial" nuclease activity.

MATERIALS AND METHODS

All the reagents, starting materials as well as solvents were purchased commercially and used without any further purification. Solvents and reagents were obtained from commercial source

and used without purification. The IR spectra (ϑ_{max}, cm^{-1}) were recorded in solid state KBr dispersion using Perkin Elmer FT-IR spectrometer. The ^{1}H-NMR spectra was recorded on Bruker-Avance 500 MHz spectrometer. The chemical shifts were reported in δ/ ppm relative to TMS. The mass spectra were recorded on using a Perkin Elmer PE-SCIEX-API 2000 mass spectrometer. The reactions were monitored by Thin–layer chromatography (TLC). Melting points were determined on Polman melting point apparatus (Model No MP96) by open capillary method and are uncorrected. All the reactions were carried out under nitrogen atmosphere.

Step-1 Preparation of chloro acetic hydrazide:

To a stirred solution at ethyl chloro acetate (3mmol) in ethanol was added hydrazine hydrate (10mmol) and refluxed 12 hours the reaction mixture was diluted with ethyl acetate followed by water. The organic layer was evaporated to obtain respective chloro acetate hydrazides the yield of the products varied from (75-90 %) [7].

Step-2 Synthesis of pyridoxal chloro acetatohydrazide(PLCAH)

To a stirred solution of pyridoxal HCl (0.50 mmol) in ethanol was added the corresponding chloroacetic hydrazides (1.0 mmol) and refluxed for 5 h. The reaction medium was poured into water and extracted with ethyl acetate. The organic layer was washed with water and concentrated under reduced pressure, to obtain the pure yellow coloured solid compounds. The purity of the compounds was checked by TLC. Yields of the products varied between 75 to 85%.

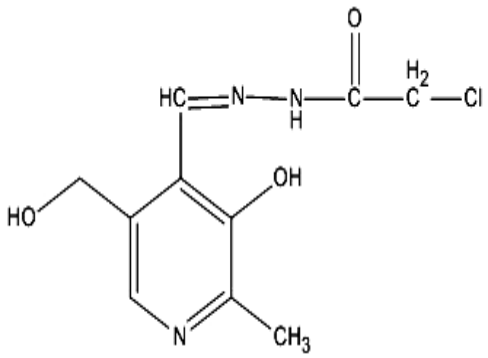

Figure 5: Structure of Pyridoxal Chloro Acetatohydrazide

Preparation of Cu (II) and Zn (II) metal complex synthesis:

Cu (II) and Zn (II) complexes of PLCAH were prepared by refluxing the metal salt solutions of zinc chloride with hot methalonic solution of ligand PLCAH for 15-20 hours. Molar ratio of metal to ligand ratio is 1:2. The pH was adjusted with ammonical buffer (pH=7). Solid complexes separated out after refluxing, which were washed with hot methanol, to remove unreacted ligand, then with DD water to remove unreacted metal salt and finally with petroleum ether. The solid complexes obtained were dried in a dessicator at room temperature.

Experimental Techniques employed to study Drug DNA Interactions:

UV-Visible absorption spectroscopy studies

Metal complex titration with calf thymus DNA

Electronic spectroscopy: The application of electronic absorption spectroscopy in DNA-binding studies is one of the mostbuseful techniques. Electronic spectra indicate the nature of interaction of complexes and DNA.

The DNA concentration per nucleotide was determined by electronic absorption spectroscopy using the known molar extinction coefficient value of 6600 M^{-1} cm^{-1} at 260 nm. Absorption titration experiments of copper(II) complex samples in buffer solution (50 mM NaCl-5 mM Tris–HCl, pH 7.2) were performed by using a fixed complex concentration to which increments of the DNA stock solutions(20,40,60,80,100µl) were added. The Ni(II) complex–DNA solutions were allowed to incubate for 10 minutes before the absorption study was carried out. 1mg of complex is dissolved in 1ml of DMSO and the concentration of the complex is found out using the formula,

$$M=0.001/\text{mol. wt of complex} \times 1000/1 = a$$

The above formula gives the initial conc. of the complex solution in 1ml DMSO. The 100 µl of this stock solution added to 3ml TRIS-HCl in a cuvette and the conc. of this solution is found out using the formula $a \times 0.1ml = x \times 3.1ml$ (x=conc. in 3ml)

The spectral data may suggest a groove mode of binding that involves a stacking interaction between the complex and the base pairs of DNA. In order to quantitatively compare the binding strength of the two complexes, the intrinsic binding constants K_b of the two complexes with CT DNA were determined according to the following equation [2] through a plot of

[DNA]/(Σa-Σf) versus [DNA]. [DNA]/(∑a-∑f) =[DNA]/(∑b-∑f) +1/Kb(∑b-∑f)) where [DNA] is the concentration of DNA in base pairs, the apparent absorption coefficient ∑a, ∑f and ∑b corresponds to Aobsd/[Ni], the extinction coefficient for the nickel complex in the free and fully bound form, respectively. In plots [DNA]/(Σa-Σf) versus [DNA] Kb is given by the ratio of slope to intercept. Intrinsic binding constants Kb of Nickel complex was obtained about 4.34 ±0.1 x 103 from absorbance data. The binding constants indicate that binds more strongly than Zn complex [8].

Electronic Absorption Titrations

Preparation of Metal Solution:

Stock solution of metal 1 gm in 1 ml DMSO from this 100 ml has to be diluted with 3 ml of Tris HCl buffer / phosphate buffer.

2. Keep D.D. water in refraction and Tris HCl in sample and give base line correction.

3. Tris HCl in ref. (after remaining D.D. water) DNA with buffer in sample, check reaction of absorbance at 260 nm and 280 nm =1: 9: 1 absorbance = calculation the concentration of DNA.

4. Then Tris HCl in refraction and complex solution in sample , take absorption , then add 20 µl of DNA to both complex and Tris HCl and take absorbance after 10 min ,

Addition of DNA to both complex and Tris HCl will be: 20 µl then 40 µl , 60 µl ,80 µl , 100 µl

Viscosity Studies:

1. Preparation of metal solution:

Stock solution of metal 1 gm in 1 ml DMSO from this 100 ml has to be diluted with 3 ml of Tris HCl buffer / phosphate buffer.

2. Keep D.D. water in refraction and Tris HCl in sample and give base line correction.

3. Tris HCl in ref. (after remaining D.D. water) DNA with buffer in sample, check reaction of absorbance at 260 nm and 280 nm =1: 9: 1 absorbance = calculation the concentration of DNA.

4. Fill Viscometer with buffer only (10 ml). Record time 3 times and take average. To above Viscometer add DNA 100 µL. Repeat the process same as above. To this solution add Ethidium bromide in intervals of 20, 40, 60, 80, 100 µL and record the readings 3 times after each addition and take the average.

5. Fill the Viscometer with buffer 10 mL followed by DNA 100 µL and add complex solution in the intervals of 20, 40, 60, 80, 100 µL and record the readings 3 times after each addition and take the average. Record time 3 times and take average.

$\eta'sp/ \eta sp = \{(t\ complex\text{-}to) / to\} / (t\ control\text{-}to) / t_o$

RESULTS:

Characterization of Ligand:

LC-MS:

The liquid chromatographic of PLCAH showed single peak indicating purity of the complex the retention time of 0.755.

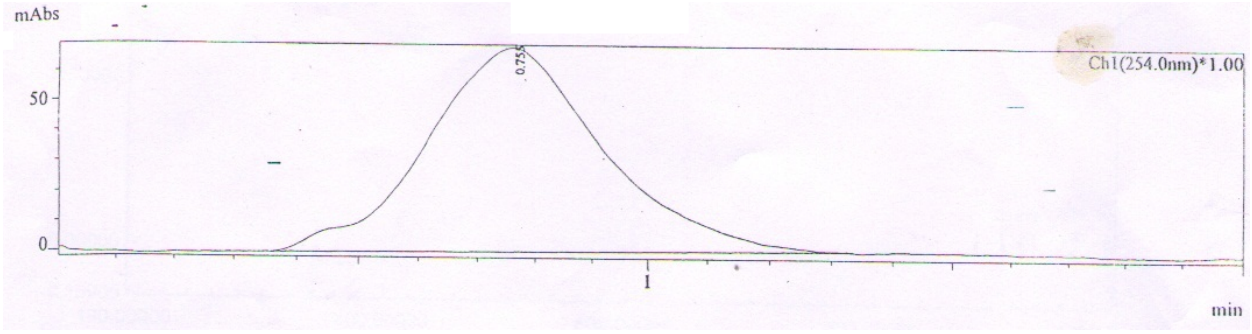

Figure 6: LC-MS of Ligand (PLCAH)

Mass spectrum showed peaks at m/z 257 [$C_{10}H_{12}N_3O_3Cl$, M^+] indicating the molecular ion

International Journal of Research
Available at https://edupediapublications.org/journals
p-ISSN: 2348-6848
e-ISSN: 2348-795X
Volume 03 Issue 14
October 2016

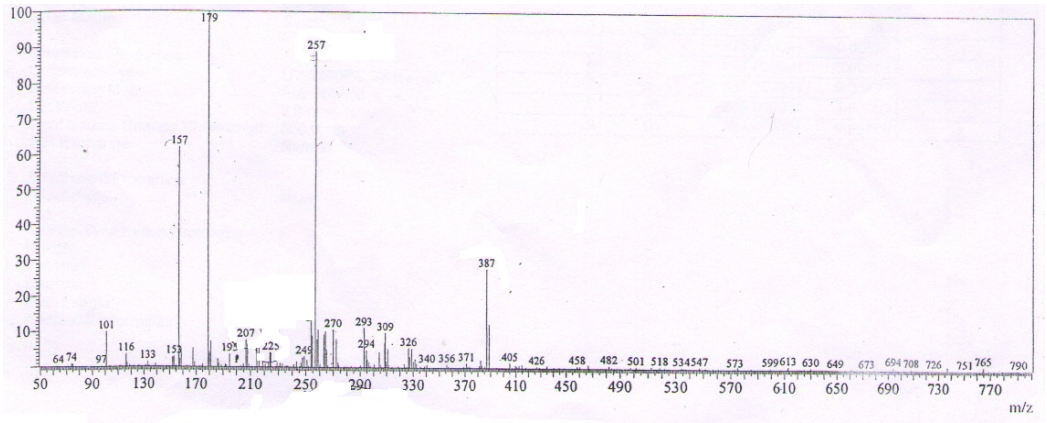

Figure 6. Mass Spectrum of Ligand (PLCAH)

IR spectrum:

The IR spectrum of PLCAH showed the following peaks at υ 3323 cm^{-1} (OH on the pyridine ring), peak at υ 3111 cm^{-1} (secondary amide-NH), υ 1750 cm^{-1} (C=O), azomethine (C=N) peak at υ 1608 cm^{-1}, peak at υ 972.12 cm^{-1}(N-N).

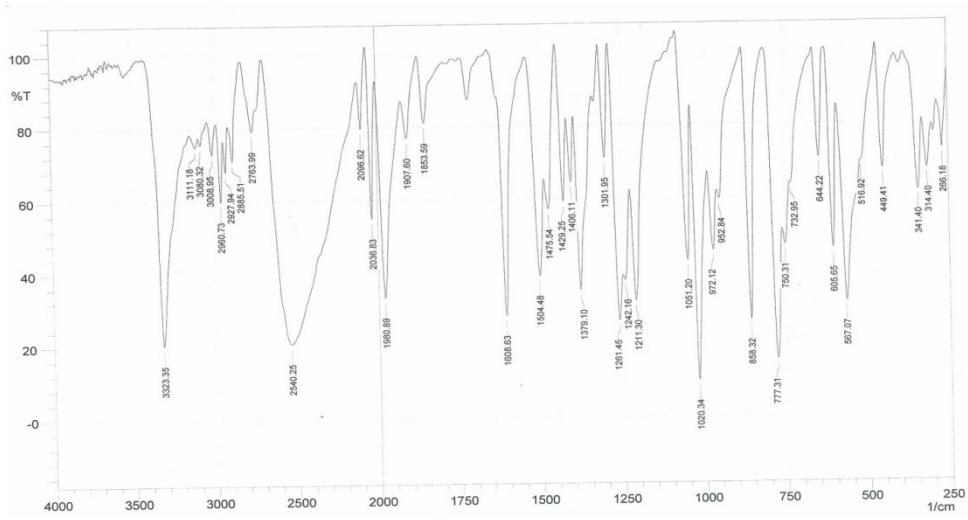

Figure 7. IR Spectrum of Ligand(PLCAH)

^{1}H-NMR of ligand:

Chemical shift of –OH present on the pyridine ring at 9.431ppm, –NH proton of 8.11 ppm aromatic (Ar H) at 6.0ppm, - CH_2OH proton at 4.764 ppm, -CH_2 proton at 2.5 ppm, -CH_3 proton at 2.0 ppm.

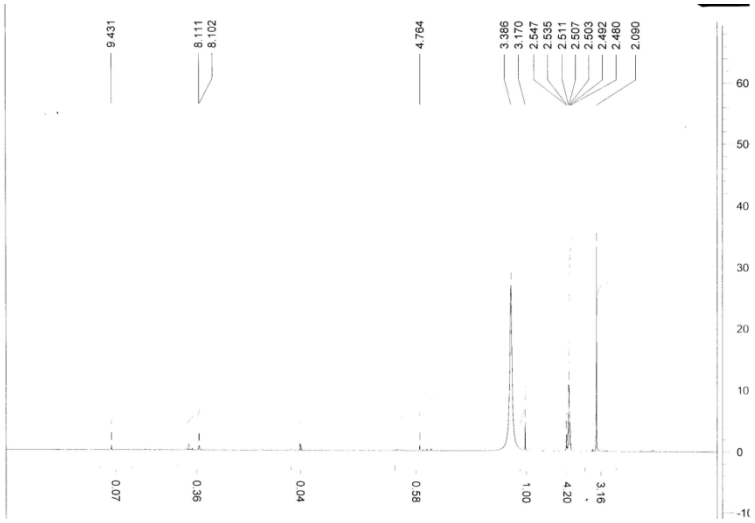

Figure 8: H-NMR of Ligand (PLCAH)

UV spectra:

The UV spectrum (Fig-5) showed peak at 285nm and 252nm which correspond to π→π* and n→π* transition of the C=O group. The band at 340nm is due to C=N group [9].

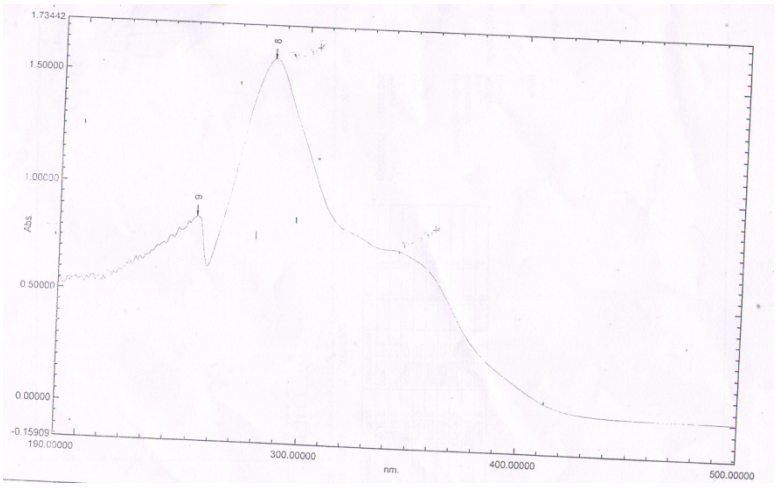

Figure 9: UV Spectra of Ligand (PLCAH)

Characterization of metal complexes

IR spectra:

Compound	υ Pyridine ring	2 ° amide	υ (C=N)	υ (C=O)	υ (N-N)

	(OH)				
PLCAH	3323	3111.18	1680.63	1750	972.12
Zn -PLCAH	———	3105.90	1575	1622.13	959.76
Cu-PLCAH	———	3100	1602.85	1680.00	954.76

The IR spectrum of Zn-PLCAH complex showed the following characteristic peaks. The peak at 3323 cm^{-1} disappeared in the complex which corresponds to Pyridine ring (OH) was present in the ligand, this indicates the coordination through oxygen. The peak at 1750 cm^{-1} decreased to 1622 cm^{-1} which corresponds to C=O indicating its coordination through oxygen. The decrease in the stretching frequency of azomethine (C=N) from 1680 cm^{-1} to 1575 cm^{-1} shows the coordination through the nitrogen. The peak at 3111 cm^{-1} decreased to 3105 cm^{-1}. The broad peak at 3300 cm^{-1} indicates coordinated water molecule. In the far-IR region peaks corresponding to M-O at 400 cm^{-1} and M-N at 350 cm^{-1} appeared in the complex spectrum [10].

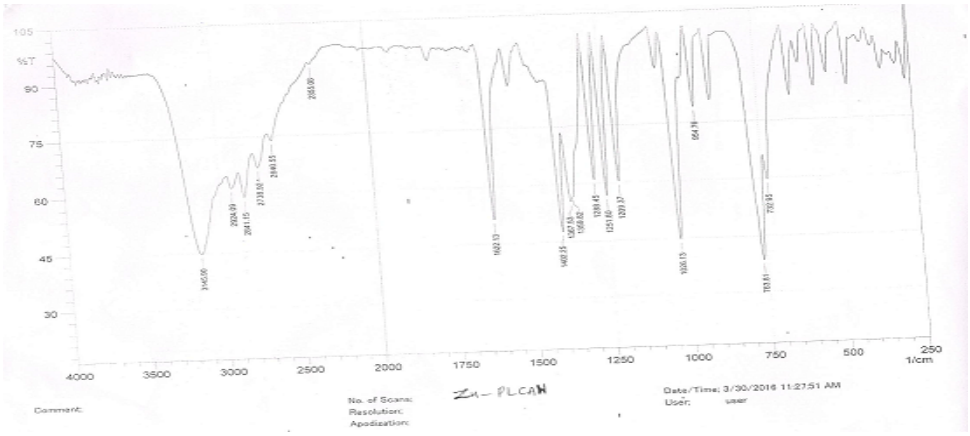

Figure 10: IR Spectrum of Zn – PLCAH

The IR spectrum of Cu-PLCAH complex showed the following characteristic peaks. The peak at 3323 cm^{-1} disappeared in the complex which corresponds to Pyridine ring (OH) was present in the ligand, this indicates the coordination through oxygen. The peak at 1750 cm^{-1} decreased to 1680 cm^{-1} which corresponds to C=O indicating its coordination through oxygen. The decrease in the stretching frequency of azomethine (C=N) from 1680 cm^{-1} to 1602 cm^{-1} shows the coordination through the nitrogen. The peak at 3111 cm^{-1} decreased to 3100 cm^{-1}. The

broad peak at 3300 cm^{-1} indicates coordinated water molecule. In the far-IR region peaks corresponding to M-O at 400 cm^{-1} and M-N at 350 cm^{-1} appeared in the complex spectrum.

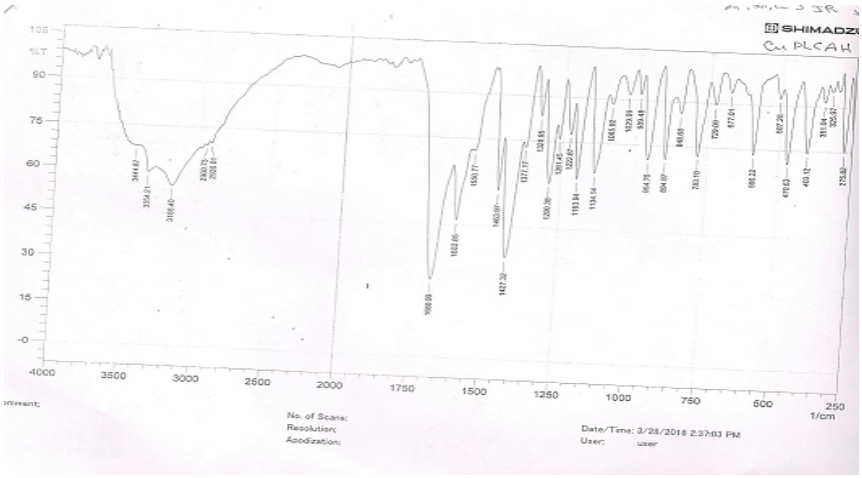

Figure 11: IR Spectrum of Cu - PLCAH

TGA:

The Cu –PLCAH complex decomposed in 3 stages. The decomposition in the range of 80˚C - 120˚C corresponds to loss of one water molecule. The loss of three water molecules in the range of 120˚C - 300˚C is indicated. Residue range is 59.5% which corresponded to undecomposed organic moiety

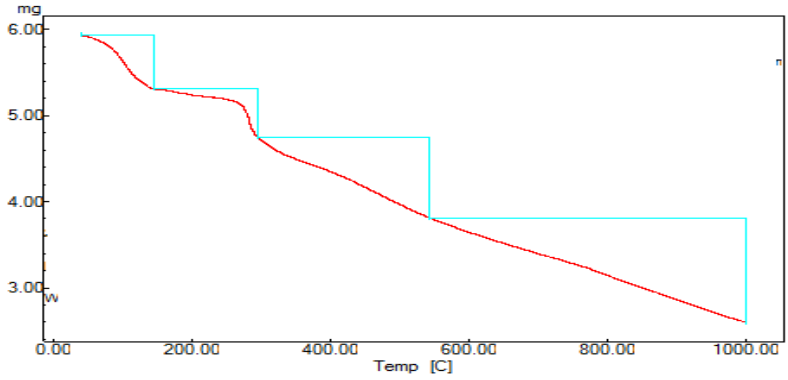

Figure 12: TGA of Cu-PLCAH

The decomposition of the Zn-PLCAH complex has been carried out in two stages there is sudden decomposition of the complex in the first stage from 30˚C – 320˚C indicating absence of water molecules. Residue range is 75- 72 % which corresponded to undecomposed organic moiety.

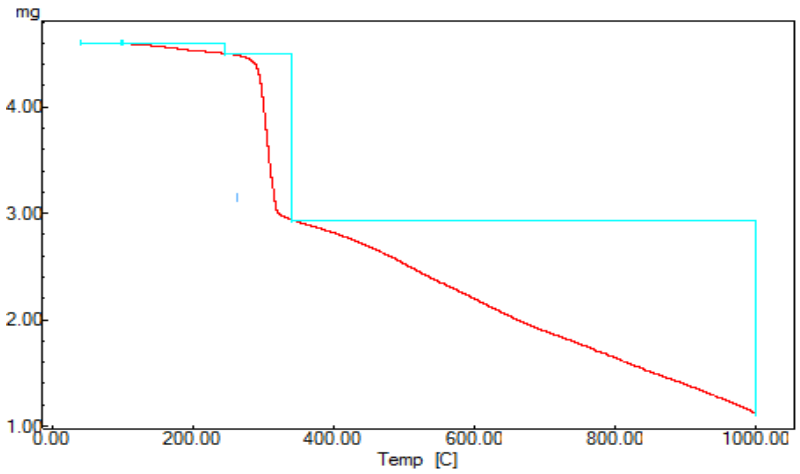

Figure 13: TGA of Zn-PLCAH

LC-MS:

The liquid chromatographic spectra of Zn –PLCAH and Cu-PLCAH complex showed single peak at 0.827 min and 0.74 min indicating purity of the complex

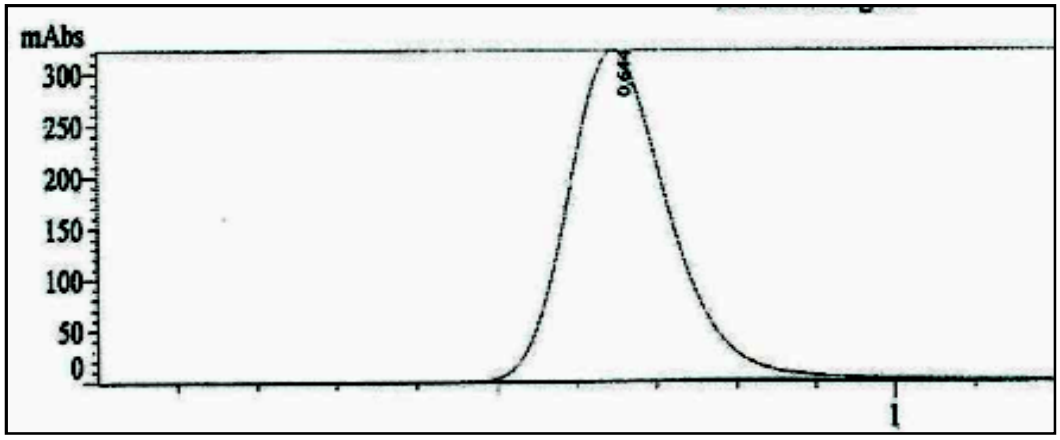

Figure 14. Liquid Chromatographic of Cu- PLCAH

Mass spectrum of Zn –PLCAH spectrum showed following peaks in its ESI (+) spectrum at m/z 578 (579.4) which corresponds to [Zn $(C_{10}H_{11}N_3O_3Cl)_2$] which indicates 1: 2 ratio of the complex. Mass spectrum of Cu –PLCAH spectrum showed following peaks in its ESI (+) spectrum at m/z 320 (320.5) which correspond to [Cu $(C_{10}H_{11}N_3O_3Cl)$] which indicates 1: 1 ratio of the complex. Peak at m/z 336 (338) which corresponds to [Cu $(C_{10}H_{11}N_3O_3Cl)$ H_2O]. Peak at m/z 356 (352) which corresponds to [Cu $(C_{10}H_{11}N_3O_3Cl)$ $(H_2O)_2$] [11].

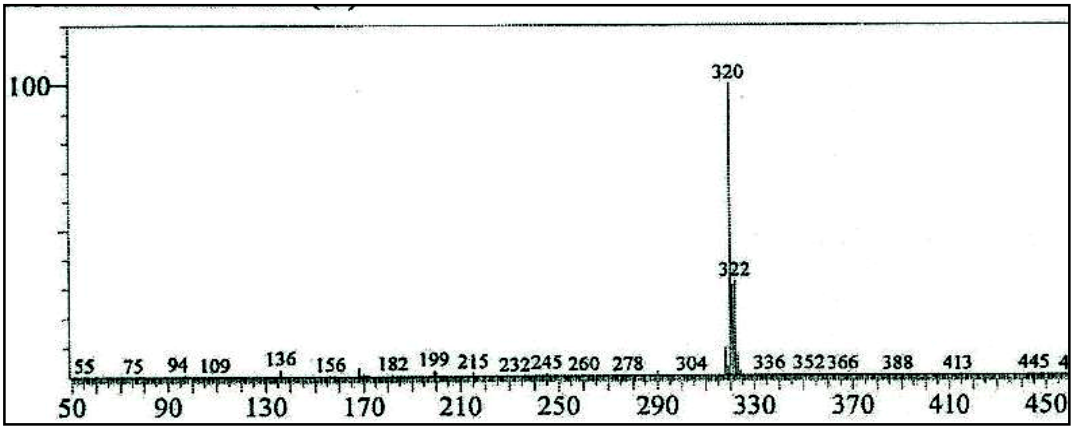

Figure 15. Mass Spectrum of Cu-PLCAH

UV spectrum

The spectrum shows a peak at 374 nm which corresponds to d-d transition [12].

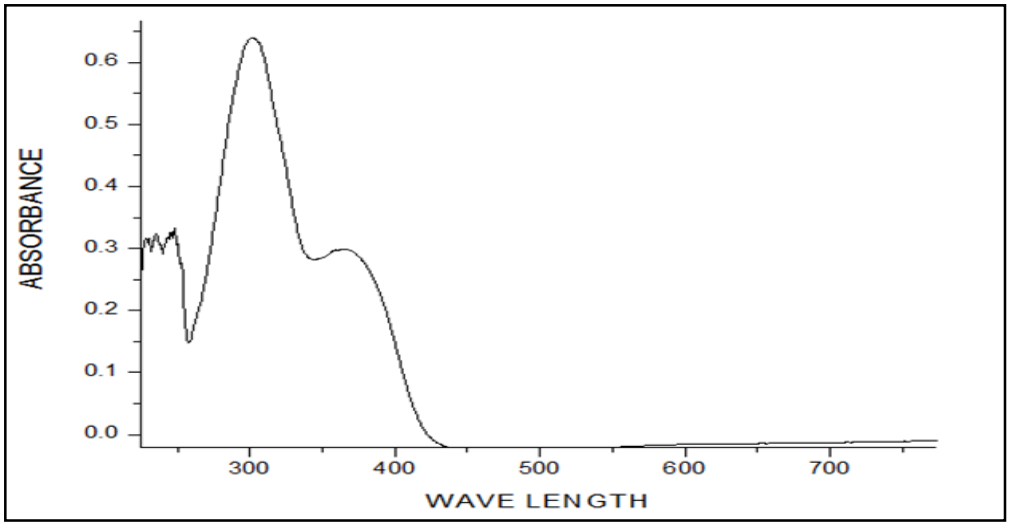

Figure 16. UV spectrum

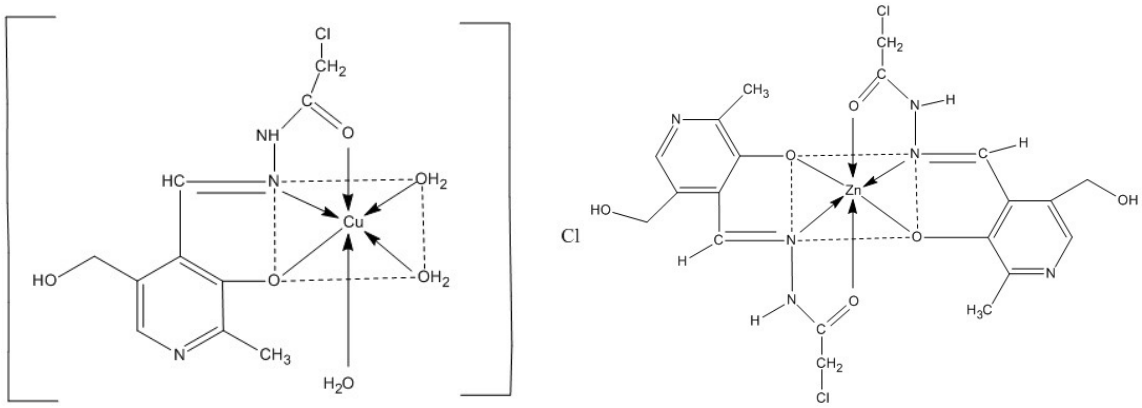

Figure 17: Tentative Structures of Complexes

Calculation of binding constant of Cu-PLACH with CT-DNA

V	E_a	E_f	$E_a - E_f$	[DNA]	[DNA]/ $E_a - E_f$
0 µl					
20 µl	12.9041731	12.72525975	0.17891335	1.836110897×10^{-6}	1.026257066×10^{-5}
40 µl	12.9041731	12.4119663	0.49267647	3.672221795×10^{-6}	7.453617168×10^{-6}
60 µl	12.9041731	12.22245371	0.68171939	5.508332692×10^{-6}	8.080058706×10^{-6}
80 µl	12.9041731	12.1990291	0.705144	7.34444359×10^{-6}	1.041552306×10^{-5}
100 µl	12.9041731	11.87640262	1.11777048	9.180554487×10^{-6}	8.213273343×10^{-6}

The binding constant of Cu-PLCAH with CT-DNA is found to be 1.9×10^{5} M^{-1}

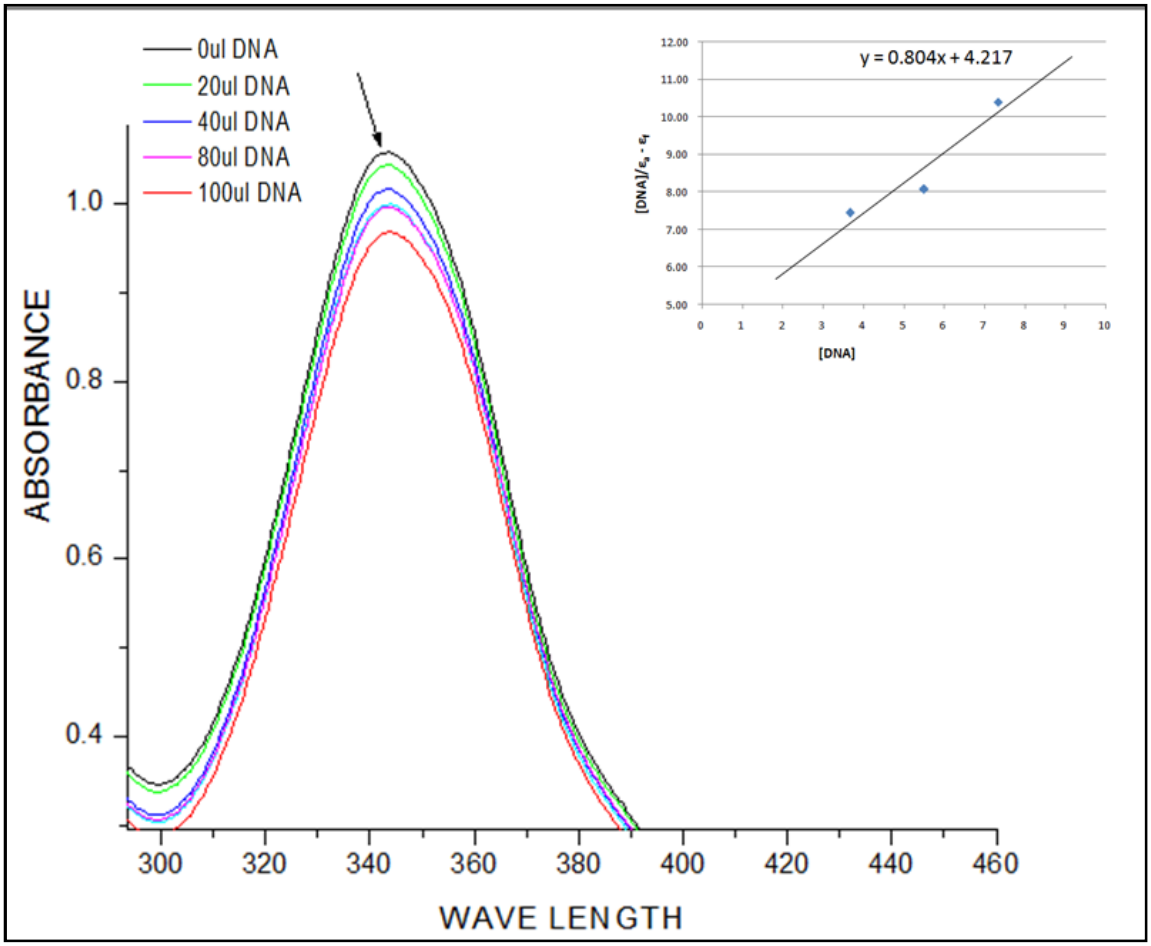

Figure 18: DNA Binding of Cu-PLACH (K_b=1.9×$10^5$$M^{-1}$)

Calculation of binding constant of Zn-PLACH with CT-DNA

Vol. of DNA	E_a	E_f	E_a-E_f	[DNA]	[DND]/E_a-E_f
0 µl					
20 µl	37.3347825	27.71544673	9.61933577	1.836110897×10^{-6}	1.908770981×10^{-7}
40 µl	37.3347825	25.73489698	11.59988552	3.672221795×10^{-6}	3.165739687×10^{-7}
60 µl	37.3347825	25.2811022	12.053680	5.508332692×10^{-6}	4.569834735×10^{-7}

80 µl	37.3347825	24.5294179	12.80536491	7.34444359×10^{-6}	5.735442638×10^{-7}
100 µl	37.3347825	24.27607204	13.05871046	9.180554487×10^{-6}	7.030215208×10^{-7}

The binding constant of Zn-PLACH with CT-DNA is 1.16×10^{6} M^{-1}

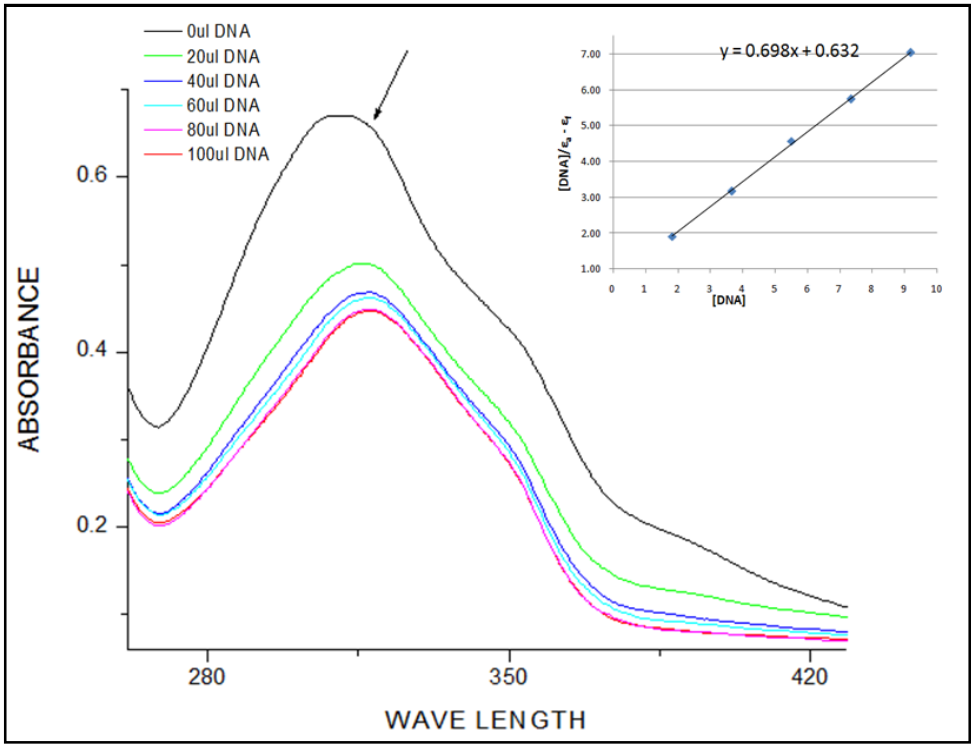

Figure 19: DNA Binding of Zn – PLCAH

Viscosity Studies:

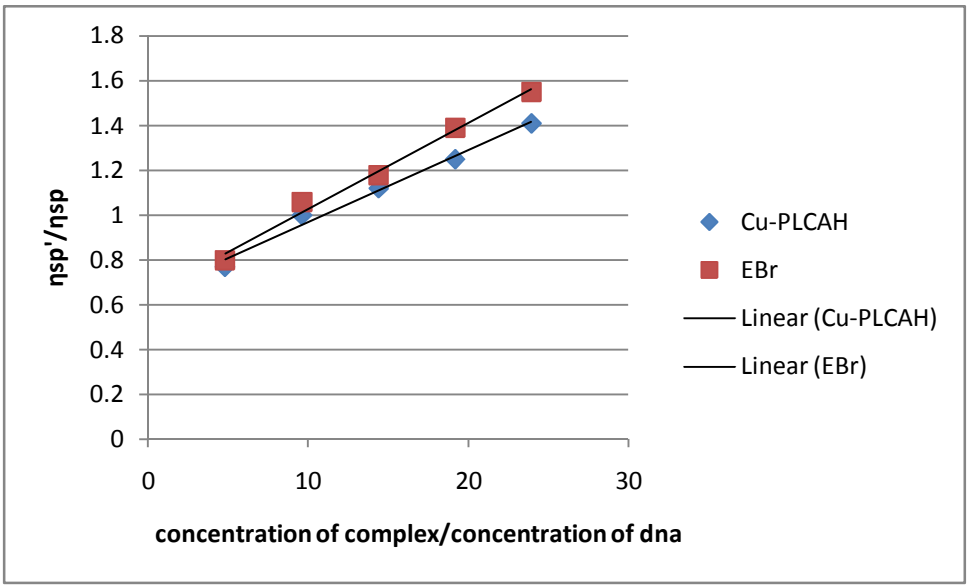

Figure 20: Viscosity studies of Cu-PLCAH

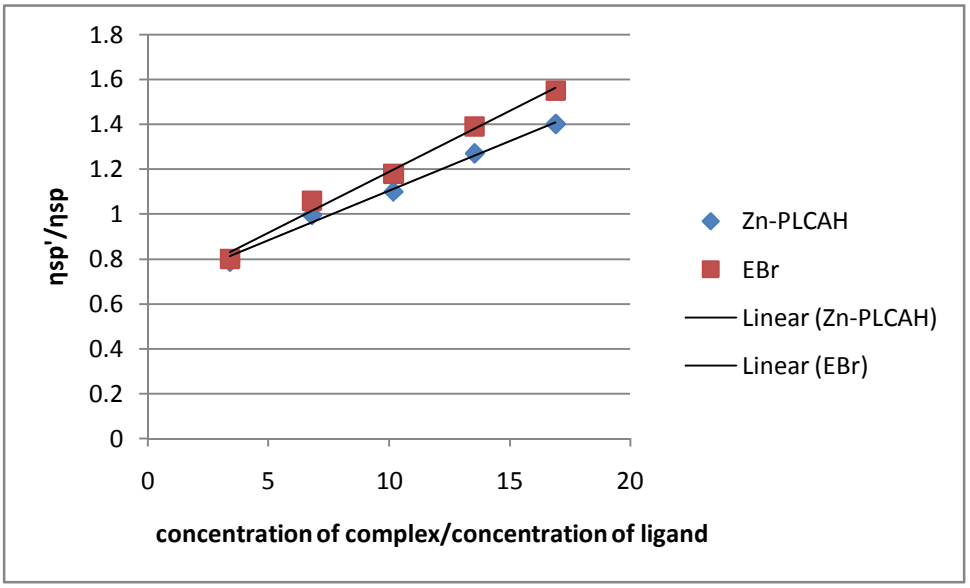

Figure 21: Viscosity studies of Zn-PLCAH

CONCLUSION:

(E-2-chloro-N-(3-hydroxy-5-hydroxymethyl)-2-methylpyridin-4yl)methylene) Acetohydrazide, a derivative of pyridoxal was synthesized by conventional method by treating Pyridoxal hydrochloride with Chloroacetic hydrazide. Cu(II) and Zn(II) metal complexes were synthesized and

characterized using LC-MS, UV, IR and TGA methods. IR spectrum of the complex revealed that the ligand coordinated through 'N' and 'O' donor atoms. The complexes were tested for DNA binding activity using Electronic Absorption spectroscopy and Viscosity measurements. The interaction of metal complexes with CT-DNA was studied and the binding constant (Kb) was calculated.

REFERENCE:

1. H. Schiff Mittheilungen aus dem universitätslaboratorium in Pisa: Eine neue reihe organischer basen Justus Liebigs Ann Chem, 131 (1) (1864), pp. 118–119
2. D.N. Dhar, C.L. TaplooSchiff bases and their applications J Sci Ind Res, 41 (8) (1982), pp. 501–506
3. P. Przybylski, A. Huczynski, K. Pyta, B. Brzezinski, F. Bartl Biological properties of schiff bases and azo derivatives of phenols Curr Org Chem, 13 (2) (2009), pp. 124–148
4. G. Bringmann, M. Dreyer, J.H. Faber, P.W. Dalsgaard, D. Staerk, J.W. Jaroszewski, et al. Ancistrotanzanine C and related 5,1′- and 7,3′-coupled naphthylisoquinoline alkaloids from Ancistrocladus tanzaniensi J Nat Prod, 67 (5) (2004), pp. 743–748
5. A.O. de Souza, F.C.S. Galetti, C.L. Silva, B. Bicalho, M.M. Parma, S.F. Fonseca, et al. Antimycobacterial and cytotoxicity activity of synthetic and natural compound Quim Nova, 30 (7) (2007), pp. 1563–1566
6. Z. Guo, R. Xing, S. Liu, Z. Zhong, X. Ji, L. Wang, et al. Antifungal properties of Schiff bases of chitosan, N -substituted chitosan and quaternized chitosan Carbohydr Res, 342 (10) (2007), pp. 1329–1332
7. Y. Zheng, K. Ma, H. Li, J. Li, J. He, X. Sun, et al.One pot synthesis of imines from aromatic nitro compounds with a novel Ni/SiO2 magnetic catalyst Catal Lett, 128 (3-4) (2009), pp. 465–474
8. R.B. Moffett N. Rabjohn (Ed.), Organic syntheses, vol. 4, John Wiley & Sons, Inc., New York (USA) (1963), pp. 605–608
9. K. Taguchi, F.H. Westheimer Catalysis by molecular sieves in the preparation of ketimines and enamines J Org Chem, 36 (11) (1971), pp. 1570–1572
10. B.E. Love, J. Ren Synthesis of sterically hindered imines J Org Chem, 58 (20) (1993), pp. 5556–5557

11. G.C. Look, M.M. Murphy, D.A. Campbell, M.A. Gallop Trimethylorthoformate: a mild and effective dehydrating reagent for solution and solid phase imine formation Tetrahedron Lett, 36 (17) (1995), pp. 2937–2940
12. A.K. Chakraborti, S. Bhagat, S. Rudrawar Magnesium perchlorate as an efficient catalyst for the synthesis of imines and phenylhydrazones Tetrahedron Lett, 45 (41) (2004), pp. 7641–7644